Design of Dual ISM Bands Low Power Rectenna for Indoor Wireless Power Transfer Application

Mohd Hezri Abdullah[1*], Arjuna Marzuki[2], and Mohd Tafir Mustaffa[1]
[1] Universiti Sains Malaysia, School of Electrical & Electronic Engineering, Penang, Malaysia
[2] Wawasan Open University, School of Science and Technology, Penang, Malaysia
Email: hezri@student.usm.my; arjunam@wou.edu.my

***Abstract*—The paper concentrates on the design of a dual-band rectenna which consists of a receiving antenna, impedance matching, single-stage voltage doubler rectifier as well as a load. The rectenna is designed using HSMS 280C Schottky diodes as its main component and combined with the lumped elements, microstrip lines as well as quasi-Yagi with semi-bowtie as the driven element. The quasi-Yagi antenna with a semi-bowtie driven element is designed using Computer Simulation Technology (CST) and its Touchstone file is imported into the Advanced Design System (ADS) for simulation with the other components of the rectenna. The rectenna with an input power of −6dBm has an optimal Power Conversion Efficiency (PCE) of 32.1% while receiving a signal from the ISM 0.868GHz band transmitter and 18.8% using the input power of −7dBm at ISM 0.915GHz band. Both PCEs are obtained using 700Ω and 900Ω as load and producing minimum output voltage (V_o) of 0.3V and 0.28V respectively. The rectenna operates in both Industrial, Scientific, and Medical (ISM) 0.868GHz and 0.915GHz bands since both are unlicensed bands. The ISM 0.868GHz band is normally used in Europe while ISM 0.915 GHz band is widely used in the United States as well as Japan. The dual-band rectenna can be used for powering a power management unit such as EM8500 or AEM30300 in an indoor environment.**

***Index Terms*—Dual-band, rectenna, power conversion efficiency, single-stage voltage doubler, Industrial, Scientific, and Medical (ISM) bands**

I. Introduction

The Internet of Things (IoT) has triggered the widespread usage of wireless sensors. The emergence of the IoT creates the main issue concerning the way energy supplying. The main drawbacks of the existing battery usage are the problem of the disposal of battery waste, maintenance cost for the replacement of depleted batteries as well as the limited lifetime of the batteries.

Nowadays, the revolutionary in electronic technology has made it possible the use ultra-low powered sensor as well as replace batteries with another alternative energy source. A potential solution is by using Radio Frequency (RF) electromagnetic as a source of energy. There are two main concepts for using the RF as an energy source namely Wireless Power Transfer (WPT) and Energy Harvesting (EH) [1].

Manuscript received August 2, 2022; revised September 10, 2022; accepted October 20, 2022.
*Corresponding author: Mohd Tafir Mustaffa (email: tafir@usm.my).

The EH concept can be done by extracting the ambient RF energy and converting the RF energy into DC power. There are a variety of ambient energy sources such as thermal energy, wind energy, solar energy, tidal energy, electromagnetic energy, and many more. Those ambient energies have the potential as sources of energy harvesting systems. Unfortunately, most energy sources cannot provide power continuously for 24 hours a day except for electromagnetic energy [2].

The WPT concept involves transferring wirelessly the RF energy received by a rectenna from a dedicated RF transmitter to a device for it to operate. A typical rectenna consists of an antenna, impedance matching, rectifier, and DC pass filter as in Fig. 1.

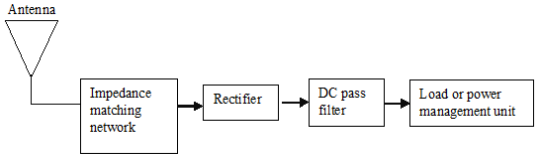

Fig. 1. A typical rectenna block diagram.

Fig. 1 shows a common topology of a rectenna. The receiving antenna will extract the RF energy and converts it to DC by using the rectifier. The impedance-matching network will ensure a maximum power transfer from the antenna to the rectifier. Generally, the capacitive and inductive elements are used in a matching network for producing a maximum delivery of power between them. The matching condition will directly reduce transmission loss. An AC-type voltage at the output of the matching network will be converted to usable DC power. The individual components of a rectenna also have their drawbacks. For instance, most antennas will have the issue of multipath fading and interference which will directly influence the system performance. Thus, a directional antenna such as a quasi-Yagi antenna which has high directivity and gain shall be used.

Currently, the quasi-Yagi antenna is being used in various applications such as personal area networks [3], [4], point-to-point comm [5], and radar applications [6].

However, the existing quasi-Yagi antenna has narrow bandwidth characteristics which restrict its usage. Nowadays, some wideband quasi-Yagi antennas have been proposed such as in [7], [8], and [9]. Unfortunately, these antennas need either complex driven element or balun. Both complex properties will directly contribute to the difficulty in fabricating the antenna as well as the bigger size of the antenna itself.

doi: 10.18178/ijeetc.12.1.60-70

Regarding other rectenna main components such as rectifiers, many types of rectifiers have been designed such as single-band rectifiers [10], dual-band rectifiers [11], [12], multiband rectifiers [13], and broadband rectifiers [14], [15]. All the respective rectifiers are designed for their specific application. Other components such as impedance matching and output filter will be designed accordingly based on the input impedance of the rectifier and the antenna.

The design of a complete rectenna system using a specified load in a WPT environment is quite scarce nowadays. The scenario occurs even though the study on the topic is progressing well [16].

A possible reason for the situation is due to the challenge of balancing critical requirements such as small form factor, low cost, high power conversion efficiency (PCE), and complying with specified regulations [16].

The objective of this study is to design a rectenna using a single-stage voltage doubler fed using a quasi-Yagi antenna with semi-bowties as driven elements. The objective is based on the requirement of the cold start input voltage needed by a power management unit such as EM8500 [17], [18] or AEM30300 [19] as well as aiming for considerably high PCE of the rectenna at the specified ISM 0.868GHz and 0.915GHz bands.

In this work, the rectenna has been designed and characterized for operating in both bands for supplying DC voltage to a power management chip (PMU) or low-powered wireless sensors. The system will be used in an indoor environment such as a smart home or hall [20].

Both unlicensed ISM bands are chosen due to having the characteristics of a good trade-off between the free-space losses and the covered range. In addition, the selected ISM bands are unlicensed bands that are suitable for being used in an indoor wireless power transfer system. The designed rectenna must operate at ISM 0.863GHz to 0.870GHz and 0.902GHz to 0.928GHz. The planar quasi-Yagi with the semi-bowties driven elements is chosen as receiving antenna of the rectenna due to its good directivity, compactness dimension, ease of fabrication as well as broadband characteristics [21], [22]. The final designed rectenna is made of a quasi-Yagi with semi-bowties as driven elements, a single-stage voltage doubler, and an impedance matching between both components.

This paper is divided into six main sections starting with the Introduction section. Section II is about an overview of the rectenna design. Section III explains the selected antenna design. Section IV delves into rectifier design. Section V elaborates on the rectenna results and their analysis. Finally, Section VI concludes the paper.

II. Overview of Rectenna and Its Topology

In this work, the rectenna is made of a rectifier consisting of Schottky diodes HSMS 280C in a single-stage voltage doubler configuration as in Fig. 1. The DC power will be used directly for energizing low-power devices or storing them in an energy storage unit. For example, the storage unit shall allow uninterrupted delivery of power to load or is used as a backup reserve whenever the required energy is not enough [18], [19]. The DC pass filter at the output section will reject the fundamentals and harmonics which are produced by the diodes. The load represents the input impedance of electronic devices such as wireless sensors or Power Management Units (PMU).

The first objective of this study is to supply sufficient DC power to a PMU such as EM8500 or AEM30300 by absorbing the RF energy from a dedicated transmitter. In line with that, a minimum of 300mV (for EM8500) or 275mV (for AEM30300) is needed for a cold start of the respective PMU. The load in Fig. 1 represents a Power Management Unit (PMU).

The EM8500 or AEM30300 is chosen to be used in this work since both devices can provide Maximum Power Point Tracking (MPPT) as well as a boost converter at its inputs. The dynamic MPPT operation of both devices can vary its input impedance according to the different input voltage from the rectifier. The rectifier usually provides insufficient DC output voltage for directly powering a sensor. The nominal operating voltage of sensors is between 1.8V and 3.3V. Hence, a PMU is needed for providing the required DC voltage to sensors. The second objective is for ensuring that the rectenna has a comparable PCE compared to other rectennas as in [15], [16].

In this work, all the rectenna components as in Fig. 1 will be integrated into the same printed circuit board. The size of the rectenna will be mainly driven by the size of the antenna. As such, the first step in designing the rectenna is by designing and characterizing the rectifier and the antenna separately. The first process is needed for ensuring a good 50Ω impedance matching as well as analyzing their characteristics respectively. The assembling of the rectifier with the antenna is the second step and the last step involves characterizing the resulting rectenna. The details of the antenna and its rectifier, low pass filter as well as the load will be discussed in the following sections.

III. Antenna Design

Microstrip technology is used for designing the antenna. The design of the antenna is explained comprehensively in [23]. In this paper, the outline of the antenna design is given for the sake of the topic's completeness. In this work, a quasi-Yagi antenna with semi-bowties as driven elements is used because it has good directional properties with sufficient bandwidth for operating in a dual-band of ISM 0.868GHz and 0.915GHz bands.

Fig. 2 shows the antenna in the form of quasi-Yagi using semi-bowties as driven elements. The antenna structure is designed on a low-loss FR4 substrate with εr = 4.6, tanδ = 0.0027, and substrate thickness =1.60mm. A feeding line width (W_f) of 3.30 mm and linefeed length (L_f) of 58 mm are used for feeding the antenna. Table I gives the detail of the antenna's dimensions.

TABLE I: FINALIZED PARAMETERS USED IN FIG. 2 [23]

Variable	Value (mm)	Variable	Value (mm)
LB_{CR}	5.60	HB_L	7.00
W_{CPL}	2.00	L_L	43.5
W_q	130.0	HB_R	7.00
B_R	47.8	L_R	43.5
L_{DD}	3.65	L_{p3}	6.60
L_{p2}	50.0	L_{DL}	42.5
LB_{CR}	6.50	L_{DR}	42.5
L_{P1}	50.0	L_D	85.0
H_{PR}	8.00	HD_L	8.60
H_{PL}	6.70	HD_R	8.60
LB_{CL}	6.50	W_{CPS}	0.50
L_f	58.0	L_G	58.0
W_f	3.30	L_{CPSR}	8.00
W_{CPR}	2.00	L_T	100.0
LT_{CL}	6.60	B_L	47.8

Note: The flare angle (θ_0) is ~ 7.22 degrees.

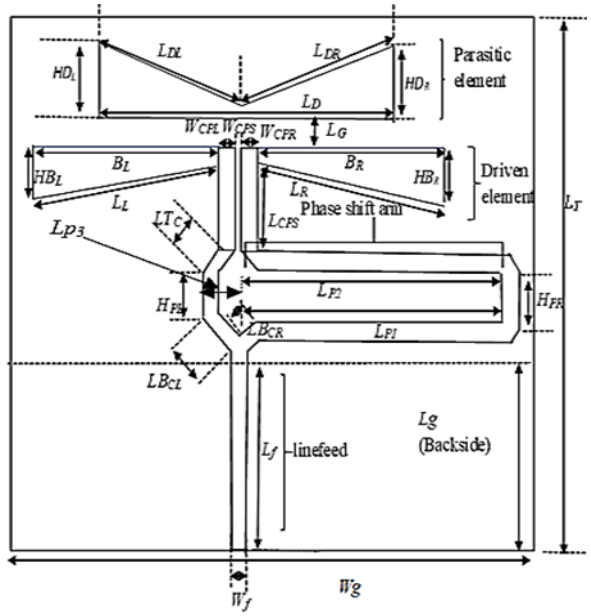

Fig. 2. The geometry of the modified quasi-Yagi antenna structure uses semi-bowtie as a driven element [23].

The antenna structure can be designed for operating on either multiple frequency bands or a single frequency. In other words, the antenna can be designed for receiving a signal from multiple or single transmitters. Most antenna designs previously were limited to a single band which is not much efficient [24], [25] and [26]. However, recent research motivation has moved on towards antenna arrays, dual-band or higher bands as well as wide bandwidth for RF energy harvesting [27], [28]. In addition, the high directive dual-band antenna for wireless applications has also gained much attention [29], [30], and [31].

The feed line has an impedance of 50Ω. The quasi-Yagi semi-bowtie antenna is selected due to its good directional properties as well as sufficient bandwidth for receiving ISM 0.915GHz (USA/Japan) and 0.868GHz (Europe) bands. The antenna is designed by applying the geometry modification of a standard quasi-Yagi of the driven element from dipole shape to semi-bowtie shape. The vital advantage of this geometry shaping is having a good bandwidth and directional characteristics suitable for the application in an indoor wireless power transfer application at both ISM bands.

There are two main methods for improving the performance of the antenna in terms of its directivity, dual-band properties, and bandwidth. The first method is by optimizing the parameters such as phase shift arms and the semi-bowtie flare angle of the antenna by using Computer Simulation Technology (CST) [23]. Secondly, the optimization of the lumped element equivalent circuit which represents the main patch of the antenna which is its driven elements. The parallel combination of capacitance (C), resistance (R), and inductance (L) are viewed as a representation of the antenna used [32], [33].

The optimization of the lumped element equivalent circuit is done in such a way that the model S-parameters match with antenna S-parameters at their resonant frequencies. In contrast, there may be a mismatch between both S-parameters since the lumped component values vary along with frequency in antenna S-parameters. On the other hand, the lumped component values are fixed in the model S-parameters [33].

Fig. 3 shows that most of the surface current concentrates at specific locations such as linefeed, coplanar stripline, left-driven element, and phase shift arms. Moreover, the shape of the semi-bowtie also contributes to minimizing the overall structure of the antenna compared to conventional quasi-Yagi [23].

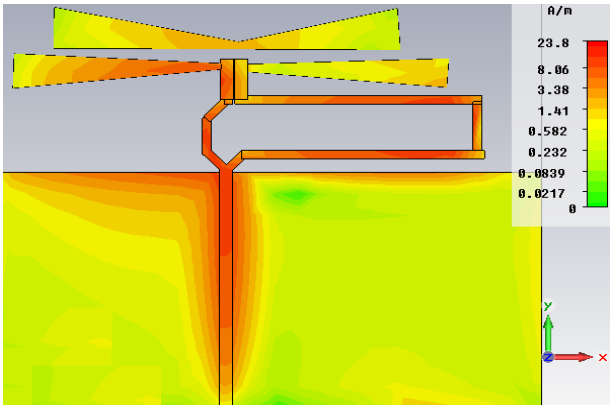

Fig. 3. Surface current distribution on the antenna structure at 0.868 GHz [23].

Theoretically, the radiation pattern and the antenna functionality depend on the surface current distribution on the antenna itself. Any changes in the geometry of the antenna shall create a new path of current as well as radiation. Hence both effects will create a new resonant frequency. Alternatively, the change in substrate material and its height will also affect the resonant frequency. From another perspective, the gain of the antenna can also be increased by increasing the height of the substrate [32].

As a pair of the semi-bowtie patch and its microstrip linefeed are conserved since it represents the biggest patch as well as the main factor contributing to the antenna characteristics, the surface current distribution will be different between the semi-bowtie patch structure and the full structure of the same antenna.

Finally, the S_{11} of the antenna result has been converted into S1P format. The aim is for integrating the antenna with its respective impedance matching and rectifier.

IV. Rectifier Design

Rectifier design is the next step in developing a rectenna. The selection of diode, impedance matching, rectifier topology, and its effects on PCE will be discussed in this section.

A. Schottky Diode Selection

The HSMS 280C is chosen as rectifying element mainly due to its low turn-on voltage and wide impedance bandwidth. Two HSMS 280C Schottky diodes are used for rectification. The Schottky diode has a low forward voltage drop (V_F) of 0.41V at 1mA forward current. The voltage drop is lower than a typical silicon diode's voltage drop between 0.6V to 1.7V [34]. The V_F limits the PCE in low input power levels. It is due to the diode needing V_F as the minimum voltage to turn on the diode itself. The diode also has lower heating losses and a very fast switching action as needed by a high-frequency incoming signal. All the properties are efficient for applications that are sensitive to accuracy [34]. The PCE saturation point of the diode relies on many parameters such as rectifier topology, the breakdown voltage of the selected diode as well as load resistance.

PCE is obtained by using (1) and (2). The variables used in (1) and (2) are V_o which represents the output DC voltage, R_L is the applied load resistance, P_o as the output power, η as its PCE, and P_{in} is the input power.

$$P_o = \frac{V_o^2}{R_L} \tag{1}$$

$$\eta = \frac{P_o}{P_{\text{in}}} 100\% \tag{2}$$

B. Impedance Matching

The heart of a rectenna is the rectifier. The rectifier determines the power conversion efficiency of the rectenna system. Theoretically, there are two main reasons for a reduction in PCE during a power transmission such as impedance mismatch between the rectifier and the antenna as well as leakage in the variety of components used.

An impedance-matching network will act as a low-pass filter for rejecting harmonics generated by the nonlinear rectifier. The network will also ensure an identical source and load. The input impedance of the rectifier shall be matched with the antenna impedance to maximize the output voltage. Antenna impedance is a function of the RF power incidence [35]. A matching circuit is needed for matching the rectifier input impedance with the antenna impedance. The impedance matching is crucial for reducing power transmission reflection in the rectenna design. The issue happens due to the nonlinearity of the diode. In addition, the rectifier's input impedance varies with the load resistance and the input power level. Both problems cause the rectifier to be able for matching the dynamic conditions of the input signal. Lumped element matching is used for ensuring a degree of freedom in matching. An L-matching network is used in this work due to its structural simplicity. The impedance matching values are initially obtained using (3) and (4) in this study. The f_r is the resonance frequency. L_1 and C_1 are the inductor and capacitor used for the impedance matching respectively.

$$f_r = \frac{1}{2\pi\sqrt{L_1 C_1}} \tag{3}$$

The input impedance (Z_{in}) at the input of the L-network equals 50 Ohm:

$$jZ_{\text{in}} = \frac{j}{2\pi f_r C_1} \tag{4}$$

The value of C_1 and L_1 are obtained by using (3) and (4) at the respective frequency. Then, the values are optimized using Smith Chart Utility. Finally, the impedance-matching values are optimized in the schematics by using the ADS simulator. The best possible matching network values (C_1 and L_1) will provide the best input return loss (S_{11}).

C. Rectifier Topology

Generally, there are myriad topologies of rectifiers in the field of RF harvesting. The main difference among them depends on the position as well as the number of diodes used. Nowadays, the series or shunt-mounted single diode is the simplest rectifier topology. Voltage doubler and voltage multiplier are normally used for improving the output DC voltage [36].

The selection of the rectifier's number of stages is very important for ensuring the required output voltage can be obtained with minimum losses due to diodes' non-linear properties. Thus, a single-stage voltage doubler [37] is used in this work. The selection is done based on the required output voltage and optimum PCE. In addition, parasitic losses of non-linear devices will increase by increasing the number of stages [37].

Based on Fig. 4, let V_{ant} be the sinusoidal input voltage, V_{antmax} the maximum sinusoidal input voltage, ω the angular frequency, and t the time, we have

$$V_{\text{ant}} = V_{\text{ant max}} \sin \omega t \tag{5}$$

Finally, the output voltage (V_{C3}) is obtained by

$$V_{C_3} = 2V_{\text{ant max}} - 2V_d \tag{6}$$

where V_d represents the forward bias voltage of the diode.

From (2), the input power P_{in} and input current I_{in} of the rectifier can be developed as

$$P_{\text{in}} = V_{\text{ant}} I_{\text{in}} \tag{7}$$

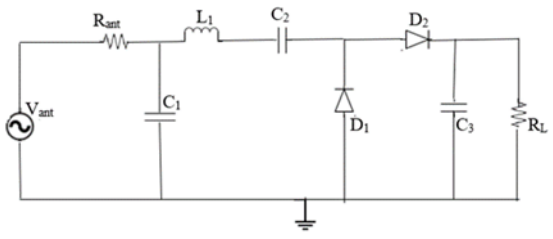

Fig. 4. A single-stage voltage doubler topology.

D. Output DC Low Pass Filter

The last step in designing the rectenna circuit is designing a low-pass filter at the output. The low pass filter is used for smoothing the signal and removing any unwanted noise. A capacitor is used for implementing the filter in ADS. Based on Fig. 4, the output capacitor (C_3) value is obtained by using (8) whereby R_L represents the load connecting to the rectifier's output.

$$C_3 = \frac{1}{2\pi f_r R_L} \tag{8}$$

In this work, Schottky diodes, lumped elements, and resistive loads are used for RF-to-DC voltage conversion. All the respective components of the rectenna are connected using an impedance-matching network for maximum power transfer. Generally, a good rectenna has a good dynamic range, low power consumption as well as good power sensitivity [38].

The rectifier is capable of converting the received RF signal into a useful DC power. The parameters of the FR4 substrate used in this work are such as substrate thickness of 1.6mm, a relative dielectric constant of 4.6, and a loss tangent of 0.02 [39]. The Harmonic Balance (HB) in the ADS software is used for simulating the circuit by considering the non-linearity properties of the Schottky diodes. The HB is used for treating non-linear circuits operated using sinusoidal excitation.

Fig. 5 reveals a schematic of the designed rectifier. The rectifier is made of Schottky diode HSMS 280C in a single-stage voltage doubler configuration. The 0.1pF is used as a low pass filter in the output section. The rectifier's L-network impedance matching is made of lumped elements consisting of an inductor (L_1) 19nH and capacitor (C_1) 3.9pF for matching the input impedance of the rectifier at both ISM 0.868GHz and 0.915GHz bands. The main parameter values at both ISM bands are as in Table II:

TABLE II: MAIN PARAMETERS USED IN FIG. 5

Component	Value
C_1	3.9pF
L_1	19nH
C_2	100pF
C_3	0.1pF
Z_{in} at 0.868GHz	(20.83-j85.3)Ohm
Z_{in} at 0.915GHz	(20.83-j80.29)Ohm
Z_o	50 Ohm

Note:
Z_{in} =Input impedance of the rectifier
Z_o = Source impedance
C_1 to C_3 and L_1 are components in Fig. 5.

All the components used at 0.868GHz are being utilized for the rectifier operating at 0.915GHz. The usage of HSMS 280C as rectifying components creates a sufficient bandwidth catering to 0.868GHz and 0.915 GHz bands.

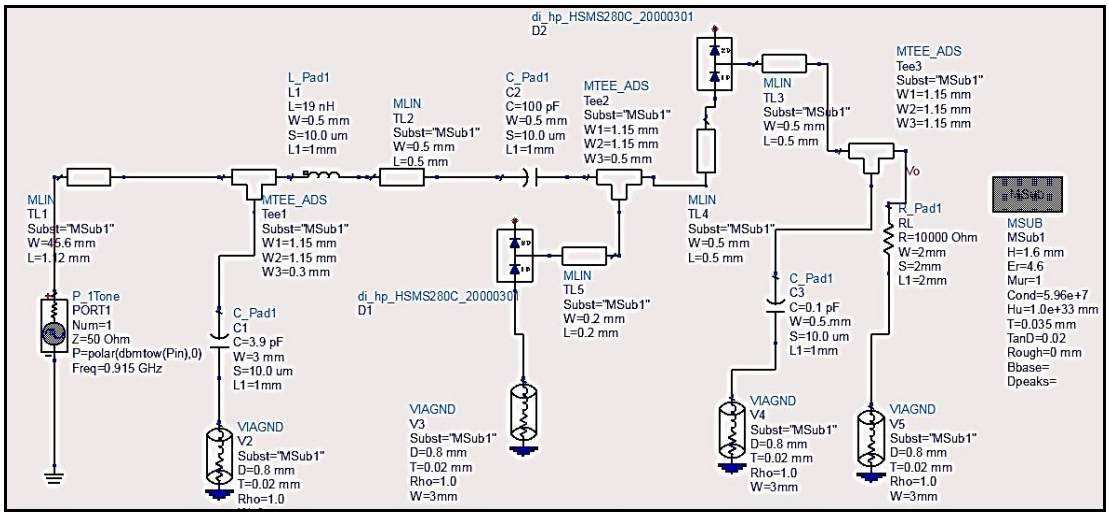

Fig. 5. Schematic of dual-band rectifier for operating at 0.915 GHz band.

The range of P_{in} is calculated by using (9), (10), and (11). The receiving antenna captures a part of the power density (S) by having an effective aperture A_r. A_r is the receiving antenna's effective aperture in the direction of the transmitter.

The received power, P_{in} is given as

$$P_{in} = A_r S \tag{9}$$

A_r can be described by (10) [20] :

$$A_r = \frac{1}{4\pi} G_r \lambda_0^2 \tag{10}$$

S is related to EIRP given as

$$S = \frac{1}{4\pi R^2} G_t P_t = \frac{\text{EIRP}}{4\pi R^2} \tag{11}$$

where λ_0 is the transmitted signal's wavelength. G_r is the gain of the receiving antenna, G_t is the gain of the transmitter, P_t is the power of the transmitter, EIRP is the effective isotropic radiated power, and R is the distance between the receiver and the transmitter.

In this work, G_r is 2.2dB [23] and EIRP is 820mW for 0.868GHz band [20] and 4W [20] for 0.915GHz.

By using (9) until (11), the P_{in} ranges at 0.868GHz and 0.915GHz bands for the practical propagation between 2m and 10m are as below:

a) $-20\text{dBm} \leq P_{in} \leq -6\text{dBm}$ for frequency of 0.868 GHz band.
b) $-13.4\text{dBm} \leq P_{in} \leq 0.53\text{dBm}$ for frequency of 0.915GHz band.

Based on both ranges, the specified P_{in} such as –6dBm and –10dBm are used at 0.868GHz band and P_{in} of 0.5dBm, –5dBm, and –10dBm are used at 0.915GHz band.

Typically, the quantity of impedance matching used in most rectifiers depends on the number of frequency bands used. The niche of the rectifier in this work is that it uses only a single impedance matching which can cover two ISM unlicensed bands. The condition happens due to the usage of HSMS 280Cs in a single-stage voltage doubler topology for being used in the configuration of the rectifier. The HSMS 280Cs have suitable properties [10] such as a large junction capacitance (C_j) as well as slow varying input impedance. The combination of the dual-band impedance matching with the rectifier using HSMS 280C has created the required dual-band characteristic in this study. The integration of both components is one of the novelties of this study.

The antenna design is one of the main novelties in this work. Hence, a quasi-Yagi antenna with semi-bowtie as driven elements has been used as receiving part of the rectenna. The quasi-Yagi antenna is chosen due to its good directional properties while the semi-bowties are used for getting the required wider bandwidth as well as the tunable directional direction based on its flare angle. In this study, the quasi-Yagi antenna has been redesigned by using semi-bowtie as driven elements for getting an exceptional property as formerly mentioned. In general, the modified quasi-Yagi antenna has the required properties of good directional properties, antenna gain as well as sufficient bandwidth for operating in dual bands of ISM 0.868GHz and 0.915GHz.

Finally, the integration of all the main components of the rectenna is being the main novelty in this study. The combination of a dual-band quasi-Yagi antenna using semi-bowtie as driven elements, dual-band impedance matching, and a dual-band rectifier represent the designed rectenna in this work. The integration of all the components has created a new chapter in the development of the rectenna since the rectenna has the capability of receiving the 0.868GHz and 0.915GHz bands simultaneously. The idea is for making a dual-band rectenna possible by using only a single antenna, a single impedance matching as well as a single rectifier. In addition, the flexibility of the rectenna in receiving the signal as well as the capability of supplying sufficient DC voltage to kickstart a power management unit has created a value-added property for the whole system. All the novelties shall be preferably in terms of overall rectenna's size, complexities, and cost.

This paper predicts that the integration of the quasi-Yagi antenna using semi-bowties as driven elements with a dual-band rectifier and dual-band impedance matching shall produce the required output voltage for powering T specific power management unit such as EM8500 or AEM30300. The rectenna shall operate at 0.868GHz and 0.915GHz for ensuring the minimum output voltage is obtained at competitive PCE compared to other rectenna systems. The same rectenna is used throughout the design. Generally, the main rectenna components such as the antenna and rectifier as well as the load will affect the obtained output voltage and PCE. In this design, the effects are stronger since semi-bowtie is used at the antenna which is very sensitive to resonant frequency [23]. In addition, the rectifier uses Schottky diodes HSMS 280C which has nonlinear properties. All the rectenna properties will be further explored in terms of its main output such as DC voltage, PCE, and input power in the following sections.

V. Rectenna Results and Discussions

The antenna has been integrated with the rectifier for producing a rectenna. An analysis approach using ADS software is used in the schematic simulation by applying Harmonic Balance as well as S parameter Simulation. As such, the circuit performance in terms of DC output voltage and conversion efficiency can be accurately predicted. The input power level is one of the main factors which will affect the conversion efficiency (η) of the rectifier since the diode has non-linear characteristics. The co-simulation of the rectifying circuit with the receiving antenna using ADS and CST is very important as part of designing a rectenna. The properties of the reflection coefficient (S_{11}) vs frequency of the antenna have been embedded in the rectifier circuit's input port using the S1P file.

Fig. 6 reveals the simulated *S*-parameter, S_{11} (return loss) value obtained by using Computer Simulation Technology (CST) software. The antenna operates at dual ISM frequency bands of 0.868GHz and 0.915GHz bands with overall bandwidth of 130MHz. Sufficient bandwidth is necessary for harvesting power at both frequency bands. The antenna is used for rectenna applications in an indoor environment. The antenna operates at the center frequency of 0.870GHz with bandwidth covering from 0.82GHz to 0.95GHz. The wide bandwidth covers both the 0.868GHz band and 0.915GHz band. The antenna suits well to be used as a receiving antenna in a rectenna system.

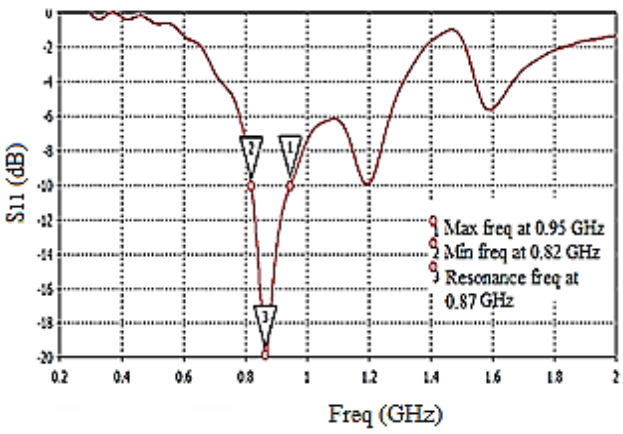

Fig. 6. Graph of S_{11} vs frequency at centre frequency 0.866GHz [23].

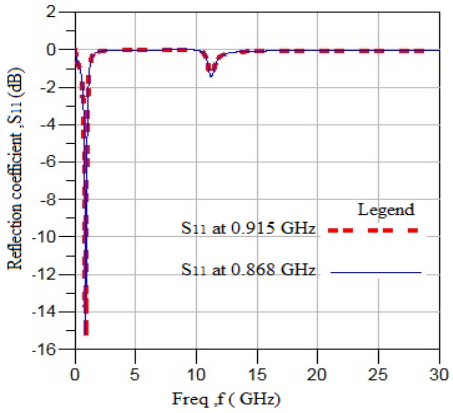

Fig. 7. Simulated reflection coefficients of the rectifier at 0.915 GHz and 0.868 GHz by using Co-simulation.

Fig. 7 shows the reflection coefficient (S_{11}) of the rectifier operating at both ISM bands. The rectifier produces similar S_{11} shapes for operating at both ISM bands. The S_{11} of both ISM bands has about the same peak value of −15.18dB at the center frequency of 0.879 GHz. The result shows that the rectifier operating at 0.868GHz and 0.915GHz have almost the same performance in terms of S_{11}. The first harmonic at 11.23 GHz has a very weak S_{11} of about −1.46dB. The weak first harmonics will not interfere with the rectifier for operating at its targeted frequency of 0.868GHz band and 0.915GHz bands.

The S_{11} information of the antenna has been exported to the rectifier schematic for co-simulation with the rest of the energy harvesting circuit as shown in Fig. 8. The Harmonic Balance and S-parameter methods are used for interpreting the relationship between its output power and the receiving antenna. The rectenna is co-simulated using the ADS and CST software. In this study, a frequency domain source is used for the rectenna simulation using ADS.

The conversion efficiency (η) of the rectenna is as

$$\eta_{\text{RF-DC}} = \frac{P_{\text{DC}}}{P_{\text{in}}} = V_{\text{DC}} \frac{V_{\text{DC}}^2}{R_L P_{\text{in}}} 100\% \qquad (12)$$

whereby P_{DC} is the output DC voltage, P_{in} is the input power, V_{DC} is the output DC voltage and R_L equals to load at the output terminal [40].

Fig. 9 demonstrates the graph of PCE vs load and V_o at specified P_{in}. The specified P_{in} such as −6dBm and −10 dBm are used in Fig. 9 (a) and P_{in} of 0.5 dBm, −5dBm, and −10dBm are used in Fig. 9 (b) for the analysis based on the calculated indoor range as in section IV.

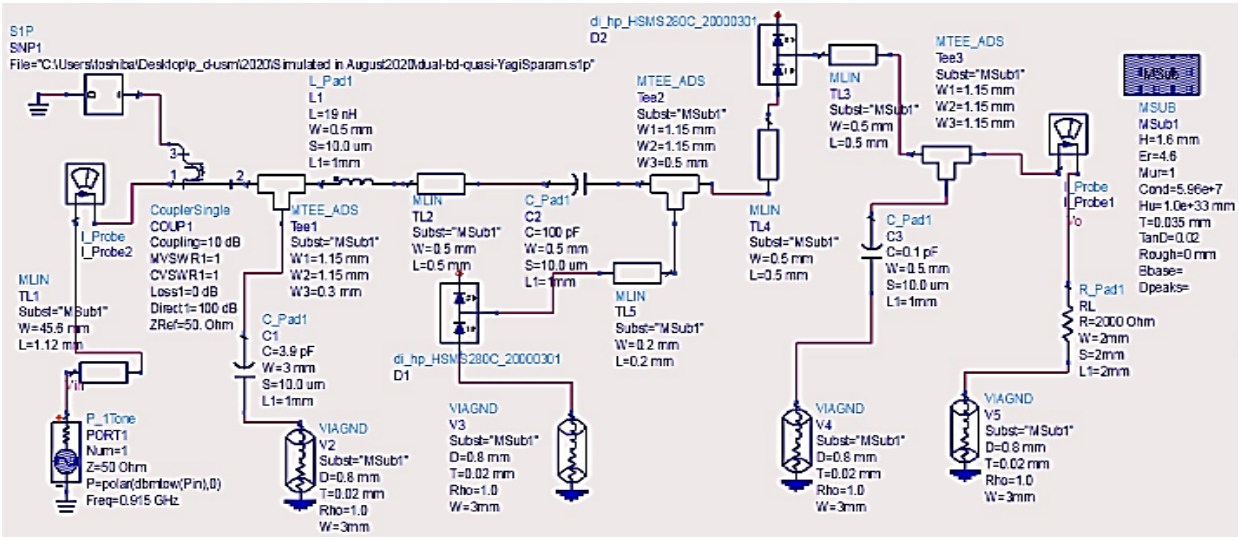

Fig. 8. Schematic of rectenna using HSMS 280C operating at 0.915 GHz bands.

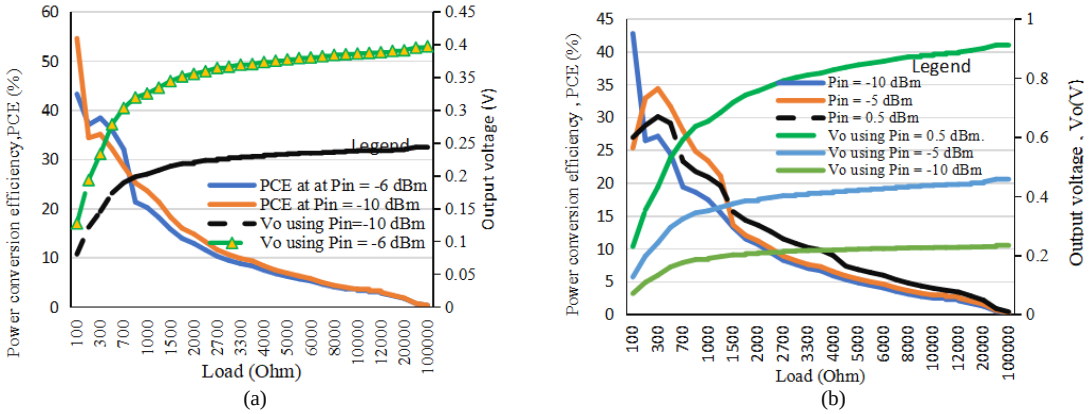

Fig. 9. Graph power conversion efficiency (PCE) and output voltage (V_o) of rectenna vs load: (a) PCE and V_o vs load at 0.868 GHz and (b) PCE and V_o vs load at 0.915 GHz

The variation of the RF-to-DC conversion efficiency (PCE) and output voltage (V_o) against load is displayed in Fig. 9 (a) and Fig. 9 (b). The graph shows that the 0.868 GHz rectenna produces an optimum PCE of 38.51% with an optimum V_o of 0.280V. The condition happens at a load of 300Ω and the P_{in} equals −6dBm.

For the 0.915GHz rectenna, the optimum PCE is 25% with V_o equals 0.345V. It is observed that the PCE is inversely proportional to load. The correlation agrees well with (9). V_o at P_{in} = −6dBm is generally higher than that at P_{in} = −10 dBm. The relationship shows that V_o is directly proportional with P_{in} which is consistent with (6) and (7) stated earlier. The rectenna received −5 dBm with load equals 900Ω. The 0.915GHz rectenna has a bandwidth (~115MHz) that covers both 0.868GHz and 0.915GHz bands. Based on Fig. 9 (a) and Fig. 9 (b), it is clear that the rectifier operating at the 0.915GHz band produces a higher maximum DC output voltage compared to that at the 0.868GHz band.

Fig. 10 depicts the graphs of PCE vs P_{in} using selected loads at both ISM bands. Both graphs show the variation in PCE vs input power. The optimum load value of 700Ω, 900Ω, and 2000Ω have been used in Fig. 10 (a) and Fig. 10 (b). Those values are chosen since a minimum output voltage of 0.3V and 0.28V can be achieved at 700Ω and 900Ω (0.868GHz band and 0.915GHz band) respectively. The 0.3V and 0.280 are the minimum cold start voltage for power management chips such as EM8500 and AEM30300 respectively. 2000Ω load is used at both frequency bands as a comparison with the optimum selected load.

The PCE is small in the low-power region due to the forward voltage of the diode being comparable to or greater than the voltage swing [35]. The generation of higher-order harmonics will also affect the PCE. If the voltage swing exceeds the breakdown voltage (V_{br}), the PCE will drop drastically. The V_{br} of the diode dictates the critical input power based on (13). Other definitions of the variables used are P_{br} which represents the breakdown power or critical input power and R_L represents the rectenna load resistance.

$$P_{br} = \frac{V_{br}^2}{4R_L} \tag{13}$$

The maximum PCE is 38.88% at P_{in} = −13dBm operating at 0.868GHz (Fig. 10 (a)). Fig. 10 (b) reveals that the max PCE of 28.6% is achieved at P_{in} = −12dBm. The 0.868GHz rectenna produces a wide input power range (~18dBm) of PCE 20% and above between -18 dBm and 10 dBm using 700Ω as load. In comparison, the 0.915GHz rectenna produces an input power range of ~10 dBm for PCE 20% and above between P_{in} −15dBm until 15dBm using 900Ω as load.

Both Fig. 10 (a) and Fig. 10 (b) demonstrate that the rectifier offers good rectifying performance and power sensitivity for low input power at the specified load. This indicates that the PCE varies with the change in P_{in}.

For example, an input signal of −6dBm shall be more appropriate for matching the rectifier with the antenna operating at the 0.868GHz band due to its high-power transmission [41]. The P_{in} = −6dBm can produce V_o of a minimum of 300mV by using 700Ω as load. The P_{in} = −5 dBm can be used with 0.915GHz band rectenna and using 900Ω as its load for getting a minimum of 300mV with optimum PCE.

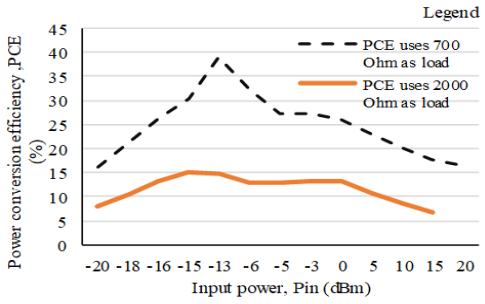

(a)

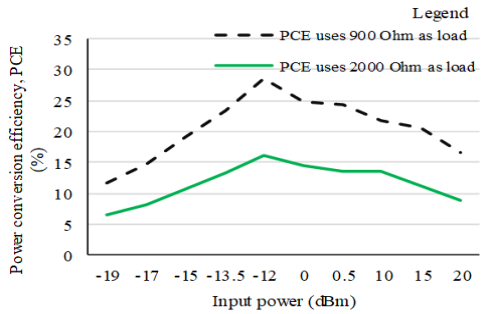

(b)

Fig. 10. Graph power conversion efficiency (PCE) of rectenna vs input power: (a) PCE vs P_{in} at 0.868GHz and (b) PCE vs P_{in} at 0.915GHz

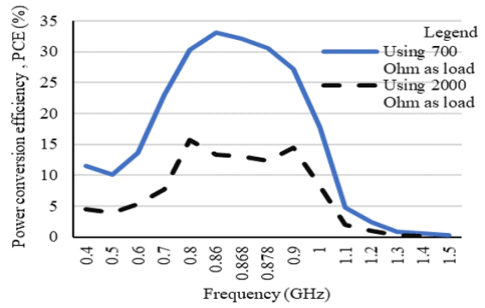

(a)

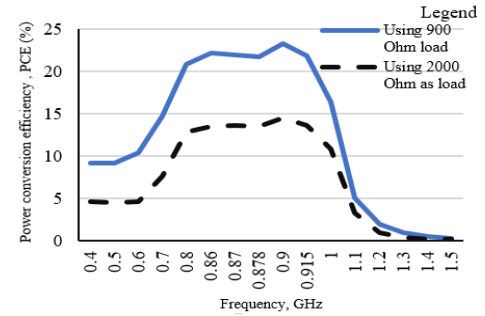

(b)

Fig. 11. Graph of PCE vs frequency: (a) PCE vs frequency with P_{in} = −6dBm and (b) PCE vs frequency with P_{in} = 0.5dBm

The selected P_{in} of −6dBm and 0.5dBm are used in Fig. 11 (a) and Fig. 11 (b). Both values represent the maximum P_{in} that can be captured by the receiving antenna based on the indoor range [20] and the type of antenna used [42]. Fig. 11 (a) and Fig. 11 (b) illustrate the graph of PCE vs frequency for ISM 0.868GHz and 0.915GHz bands. Both graphs demonstrate that both rectennas operate at the designed frequencies. Thus, the scene proves that the methodology and the theory used are correct.

Fig. 11 (a) shows that the best PCE between 25% and 33% is obtained between 0.8GHz and up to 1GHz. The PCE is a bit lower at about 20% within the same frequency range while operating at 0.915GHz.

Fig. 12 shows a reflection coefficient (S_{11}) against frequency. The figure demonstrates the characteristics of S_{11} in both ISM bands. Both P_{in} of −6dBm (at 0.868GHz) and −7dBm (at 0.915GHz) are used. The input powers are used because the values are the optimum values and comply with both objectives of this study which are getting the minimum V_o for triggering the cold start of the specified PMU and competitive PCE. Both conditions are obtained at the specified ISM bands. It is observed in Fig. 12 that both resonant frequencies at 0.868GHz and 0.915 GHz are excited with good impedance matching. The graph also indicates that the rectenna has the same pattern of S_{11} at both ISM bands but a different peak value. It is due to the rectenna using the same rectenna configuration such as impedance matching, substrate, copper tracks, and rectennas' dimensions at both ISM bands. The difference is at the transmitter which either uses ISM 0.868GHz or 0.915GHz bands or transmits both bands.

Theoretically, an efficient reception/transmission of signal at any frequency band will require a large impedance bandwidth with a good reflection coefficient (S_{11}) [32]. In this work, Fig. 12 shows a good impedance matching (S_{11} < 10dB) between 0.815GHz to 0.93GHz at both 0.868GHz and 0.915GHz bands during the co-simulation. The result shows that both the ISM 0.868 GHz and 0.915GHz frequency bands can be covered by the same rectenna. The first harmonic does happen at 9.8 GHz but has a much weaker S_{11} of −5dB. The first harmonics will not interfere with the targeted frequency bands for the rectenna at 0.868GHz and 0.915GHz bands.

Finally, based on Fig. 9, Fig. 10, Fig. 11, and Fig. 12, the best sensitivity of P_{in} for the rectenna operating at both ISM bands are −6dBm (at 0.868GHz band) and −7 dBm (at 0.915GHz band). Table III compares the rectenna with the previous designs. The designed rectenna at the 0.868GHz band has a better sensitivity than that presented in [41], [43], [44], and [45] as well as a comparable PCE compared to all the rectennas in Table III. Most of the rectennas in Table III use impedance matching such as 2 impedance matchings for 2 frequency bands while a single impedance matching for a single frequency band. Most of them use the quantity of impedance matching according to their operating frequency bands. In this work, the rectenna operates using a single dual-band impedance matching and operates at dual frequency bands. The condition happens due to the right combination of the HSMS-280C and single-stage voltage doubler topology as the rectifier main block. The V_o of the rectenna in Table III is also sufficient for triggering the specific PMU.

In this work, the dual-band rectifier, the dual-band quasi-Yagi antenna, and the dual-band impedance matching are combined for producing a rectenna. This design is comparatively using fewer components compared to most rectenna designs such as in [46] and [47]. Thus, the effects of the nonlinear properties of the Schottky diodes within the specified input power and load range can be minimized.

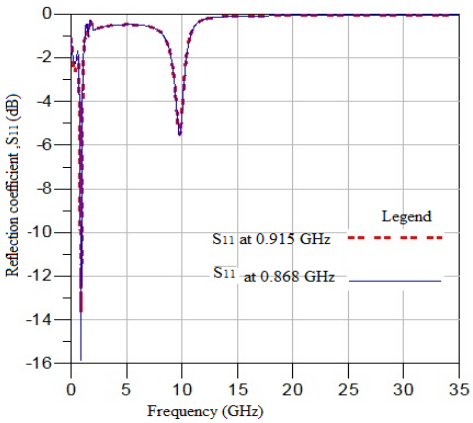

Fig. 12. Reflection coefficient (S_{11}) of the rectenna.

TABLE III: COMPARISON WITH PREVIOUS RECTENNA PERFORMANCE

Ref.	Freq (GHz)	Input power (dBm)	Single-tone, peak eff. (%)	Load (Ω)	Max. output DC voltage (V)
[41]	0.433	-5	56	4700	*NR
[43]	24	18	35	400	2.5
[44]	0.9 &2.45	0	43 and 39	500	*NR
[48]	0.86	-7	37	**PMU	0.300
[49]	0.700 and 1.4	-6.5 and -4.5	47 and 36	1900	0.700
This work	0.868 and 0.915	-6 and -7	32.1 and 18.8	700 and 900	0.300 and 0.280

*NR=Not reported
**PMU=Power management unit

VI. CONCLUSION

The novel rectenna using a dual-band modified quasi-Yagi antenna integrated with dual-band impedance matching and a dual-band rectifier has been designed successfully in this work. The required V_o (Fig. 9 (a) and Fig. 9 (b)), a competitive PCE (by referring to Table III), and wide input power (as shown in Fig. 10 (a) and Fig. 10 (b)) have been obtained by using a specific load in this study. The rectenna operating at 0.868GHz has the best sensitivity at P_{in} equals −6dBm which produces a minimum V_o of 0.3V with PCE of 32.1%. Meanwhile, the rectenna operates at 0.915 GHz and has its best at P_{in} at −7dBm producing a minimum V_o of 0.275V with a PCE of 18.8%. Both results comply with the objectives of the study for getting the minimum required V_o and competitive PCE at both ISM bands. The rectenna also has a bandwidth of about 115MHz (13.2%). The 13.2% is obtained by considering the derivation method in [50]. The 13.2% represents its bandwidth between 0.815GHz to 0.93GHz which covers both ISM bands. The bandwidth shall be just sufficient for covering both the unlicensed ISM bands. It is to avoid the bandwidth from interfering with other licensed bands. In addition, this rectenna has the advantage of using the same rectifier, impedance matching, and antenna as well as the same substrates and copper dimensions for covering both ISM bands compared to the previous literature as in Table III. The above characteristics suit well for being used in an indoor WPT application where the typical distance range of a house or hall is between 2m and 10m [20]. This study shows that the rectenna is flexible since it can operate simultaneously in the specified ISM bands.

The integration of the single-stage voltage doubler using HSMS 280C as its main component with the single impedance matching network has created a dual-band rectifier with the required bandwidth. The HSMS 280C properties which have been studied in [10] have verified the advantage of using the diode at both ISM bands. The HSMS 280C diode has the highest impedance bandwidth compared to other diodes such as HSMS 282C, HSMS 285C, and HSMS 286C. The HSMS 280C has a wide bandwidth compared to others since it has a comparatively large junction capacitance (C_j) as well as slow varying input impedance. The characteristics help in achieving wide impedance bandwidth. The integrated dual-band impedance matching with the rectifier has created the second novelty of this study.

The use of the novel modified quasi-Yagi antenna has contributed to creating a sufficient bandwidth for both ISM unlicensed bands. The modified quasi-Yagi antenna has the capability of ensuring the operating frequency is between 0.815GHz to 0.930GHz. Thus, the rectenna is suitable for powering the power management chip in an indoor environment of a house or building at both specified unlicensed bands.

CONFLICT OF INTEREST

The authors declare no conflict of interest.

AUTHOR CONTRIBUTIONS

All authors conducted the research; Mohd Hezri conducted the design and simulations using CST and Keysight ADS in the laboratory. Mohd Hezri, Arjuna Marzuki and Mohd Tafir wrote the paper. All authors had approved the final version.

FUNDING

This work was supported by Ministry of Higher Education Malaysia for Fundamental Research Grant Scheme with Project Code: FRGS/1/2019/TK04/USM/02/3.

ACKNOWLEDGMENT

The authors thank Universiti Sains Malaysia for the helpful support in terms of advice, materials, and facilities.

REFERENCES

[1] A. Costanzo and D. Masotti, "Smart solutions in smart spaces," *IEEE Microw. Mag.*, vol. 17, no. 5, pp. 30–45, May 2016.

[2] W. Saeed, N. Shoaib, H. Cheema, *et al*., "RF energy harvesting for ubiquitous, zero power wireless sensors," *Int. J. of Ant. and Propagation*, vol. 2018, pp. 1-16, Apr. 2018.

[3] M. Sun, X. Qing, and Z. N. Chen, "60-GHz end-fire fan-like antennas with wide beamwidth," *IEEE Trans. Antennas Propag*., vol. 61, no. 4, pp. 1616–1622, April 2013.

[4] L. Pazin and Y. Leviatan, "A compact 60-GHz tapered slot antenna printed on LCP substrate for WPAN applications," *IEEE Antennas Wirel. Propag. Lett.*, vol. 9, no. 9, pp. 272–275, 2010

[5] S. D. Assimonis, S. N. Daskalakis, and A. Bletsas, "Sensitive and efficient RF harvesting supply for batteryless backscatter sensor networks," *IEEE Trans. Microw. Theory Tech.*, vol. 64, no. 4, pp. 1327–1338, Apr. 2016.

[6] J. Shao, G. Fang, Y. Ji, *et al*., "A novel compact tapered-slot antenna for GPR applications," *IEEE Antennas Wirel. Propag. Lett.*, vol. 12, no. 19, pp. 972–975, Jan. 2013.

[7] Q. Awais, Y. Jin, H. T. Chattha, *et al*., "A compact rectenna system with high conversion efficiency for wireless energy harvesting," *IEEE Access*, vol. 6, pp. 35857–35866, Jun. 2018.

[8] X. Zhao, Y. Huang, X. Xue, *et al*., "A CPW-fed broadband quasi-Yagi antenna with low cross-polarization performance," *AEU - Int. J. Electron. Commun.*, vol. 83, pp. 188–192, Jan. 2018.

[9] N. M. Tarpara, R. R. Rathwa, and N. A. Kotak, "Design of slotted microstrip patch antenna for 5G application," *Int. Res. J. Eng. Technol.*, vol. 05, no. 4, pp. 2827–2832, Apr.2018.

[10] S. Agrawal, M. S. Parihar, and P. N. Kondekar, "Exact performance evaluation of RF energy harvesting with different circuit's elements," *IETE Tech. Rev. (Institution Electron. Telecommun. Eng. India)*, vol. 35, no. 5, pp. 514–522, Sep. 2018.

[11] M. S. Papadopoulou, A. Boursianis, A. Skoufa, *et al*., "Dual-band RF-to-DC rectifier with high efficiency for RF energy harvesting applications," in *Proc. 9th Int. Conf. Mod. Circuits Syst. Technol. MOCAST*, Bremen, 2020, pp. 1–4.

[12] Z. Popovic, S. Korhummel, S. Dunbar, *et al*., "Scalable RF energy harvesting," *IEEE Trans. Microw. Theory Tech.*, vol. 62, no. 4, pp. 1046–1056, 2014.

[13] U. Muncuk, K. Alemdar, J. D. Sarode, *et al*., "Multiband ambient RF energy harvesting circuit design for enabling batteryless sensors and IoT," *IEEE Internet Things J.*, vol. 5, no. 4, pp. 2700–2714, 2018.

[14] C. Song, Y. Huang, P. Carter, *et al*., "Novel compact and broadband frequency-selectable rectennas for a wide input-power and load impedance range," *IEEE Trans. Antennas Propag.*, vol. 66, no. 7, pp. 3306–3316, Jul. 2018.

[15] Y. Shi, J. Jing, Y. Fan, *et al*., "A novel compact broadband rectenna for ambient RF energy harvesting," *AEU-Int. J. Electron. Commun.*, vol. 95, pp. 264–270, 2018.

[16] J. Janhunen, K. Mikhaylov, J. Petäjäjärvi, *et al*., "Wireless energy transfer powered wireless sensor node for green IoT: Design, implementation, and evaluation," *Sensors*, vol. 19, no. 1, p. 90, Dec. 2018.

[17] J. H. Hire, N. Agianniotis, B. P. Kofoed, *et al*., "Energy harvesting in the immersed tunnel for powering wireless sensor nodes for corrosion monitoring," *IEEE Sensors Journal*, vol. 22, no.10, pp. 9892-9903, April 2022.

[18] E. M. Microelectronic, "Power management controller EM8500," EM 8500 Datasheet, May 2017.

[19] E-peas Semiconductors. Highly versatile buck-boost ambient Energy Manager Battery Charger for AC/DC Sources. AEM30300 datasheet. Jan. 2021.

[20] S. Keyrouz, "Practical rectennas: Far-field RF power harvesting and transport," Ph.D. dissertation, Faculty of Electrical Engineering, Eindhoven University of Technology, Eindhoven, The Netherlands, 2014.

[21] C. E. Capovilla, H. X. Araujo, A. J. S. Filho, *et al*., "Experimental analysis of quasi-yagi antenna shapes," *Przegl Ad Electrotechniczny (Electrical Review)*, vol. 89, no. 12, pp. 100–104, Dec. 2013.

[22] O. Amjad, S. W. Munir, Ş. T. Imeci, *et al*., "Design and implementation of dual-band microstrip patch antenna for WLAN energy harvesting system," *Appl. Comput. Electromagn. Soc. J*., vol. 33, no. 7, pp. 746–751, July 2018.

[23] M. H. Abdullah, A. Marzuki, and M. T. Mustaffa, "Design of unlicensed dual band quasi-yagi antenna using semi-bowtie for indoor wireless power transfer application," *J. of Commun*., vol. 16, no. 12, pp. 535–544, Dec. 2021.

[24] M. K. A. Rahim, M. Z. A. A. Aziz, and C. S. Goh, "Bow-tie microstrip antenna design," in *Proc. 13th IEEE Int. Conf. on Networks Jointly Held with the 2005 IEEE 7th Malaysia Int. Conf. on Communic*, Kuala Lumpur, 2005, pp. 17–20.

[25] C. Guo and R. C. Liu, "A 900MHz shielded bow-tie antenna system for ground penetrating radar," in *Proc. of the XIII Int. Conf. on Ground Penetrating Radar*, Lecce, 2010, pp. 1-6.

[26] A. Zabri, M. K. A. Rahim, F. Zubir, *et al*., "Fractal Yagi-Uda antenna for WLAN applications," *Telkomnika*, vol. 17, no. 5, pp. 2155–2160, Oct. 2019.

[27] D. H. Sadek, H. A. Shawkey, and A. A. Zekry, "Compact and high-efficiency rectenna for wireless power-harvesting

applications," *Int. J. of Ant. and Propagation*, vol. 2021, pp. 1-8, Dec. 2021.
[28] Y. Bakirli, A. Selek, and M. Secmen, "Broadband compact quasi Yagi antenna for UHF wireless communication systems with enhanced performance at UHF ISM bands," *Radioengineering*, vol. 29, no. 3, pp. 460–470, 2020.
[29] V. G. Kasabegoudar and S. Shirabadagi, "Quasi Yagi antennas for the state of the art applications," *Int. J. of Engineering Trends and Technology*, vol. 70, no. 4, pp. 1–14, Apr. 2022.
[30] M. H. Hoang, H. P. Phan, T. Q. V. Hoang, *et al*., "Efficient compact dual-band antennas for GSM and Wi-Fi energy harvesting," in *Proc. Int. Conf. on Advanced Technologies for Communications*, Hanoi, 2014, pp. 401–404.
[31] D. G. Patanvariya and A. Chatterjee, "A compact bow-tie shaped wide-band microstrip patch antenna for future 5G communication networks," *Radioengineering*, vol. 30, no. 1, pp. 40–47, Apr. 2021.
[32] B. Mishra, V. Singh, and R. Singh, "Gap coupled dual-band petal shape patch antenna for WLAN/WiMAX applications," *Adv. Electr. Electron. Eng*., vol. 16, no. 2, pp. 185–198, June 2018.
[33] A. Nella and A. Gandhi, "Lumped equivalent models of narrowband antennas and isolation enhancement in a three antennas system," *Radioengineering*, vol. 27, no. 3, pp. 646–653, Sept. 2018.
[34] H. Sun, Y. X. Guo, M. He, *et al*., "Design of a high-efficiency 2.45-GHz rectenna for low-input-power energy harvesting," *IEEE Antennas Wirel. Propag. Lett*., vol. 11, pp. 929–932, Aug. 2012.
[35] K. S. Divakaran, K. Deepti, and Nasimuddin, "RF energy harvesting systems: An overview and design issues," *Int. J. RF Microw. Comput. Eng.*, vol. 29, no. 1, pp. 1–15, Jan. 2019.
[36] F. Sari and Y. Uzun, "A comparative study: Voltage multipliers for RF energy harvesting system," *Commun. Fac. Sci. Univ. Ank. Series A2-A3*, vol. 61, no. 1, pp. 12–23, Feb.2019.
[37] M. H. Abdullah, A. Marzuki, and M. T. Mustaffa, "Design of high-efficiency voltage doubler for energy harvesting application," in *Proc. 8th Int. Conf. on Computer and Communication Engineering Design*, Kuala Lumpur, 2021 pp. 284–287.
[38] S. Divakaran, D. D. Krishna, Nasimuddin, *et al*., "Dual-band multi-port rectenna for rf energy harvesting," *Prog. Electromagn. Res. C*, vol. 107, pp. 17–31, Oct. 2020.
[39] R. L. R. D. Silva, S. T. M. Gonçalves, C. Vollaire, *et al*., "Analysis and optimization of ultra-low-power rectifier with high efficiency for applications in wireless power transmission and energy harvesting," *J. Microwaves, Optoelectron. Electromagn. Appl*., vol. 19, no. 1, pp. 60–85, Mar. 2020.
[40] M. A. Sennouni, B. Abboud, and A. Tribak, "Circular polarized C-band rectenna design for enhanced RF power harvesting," presented at the 1st International Conference on Computing Wireless and Communication Systems (ICCWCS-2016), Settat, Morocco, November 2016.
[41] J. Wei Zhang, X. Bai, W. Yang Han, *et al*., "The design of radio frequency energy harvesting and radio frequency-based wireless power transfer system for battery-less self-sustaining applications," *Int. J. RF Microw. Comput. Eng.*, vol. 29, no. 1, e21658, Jan. 2019.
[42] Antenna Theory Analysis and Design, 4th ed., John Wiley & Sons, Hoboken, New Jersey, 2016, pp. 783-798
[43] B. T. Malik, V. Doychinov, A. M. Hayajneh, *et al*., "Wireless power transfer system for battery-less sensor nodes," *IEEE Access*, vol. 8, pp. 95878–95887, May 2020.
[44] A. M. Jie, N. Nasimuddin, M. F. Karim, *et al*., "A dual-band efficient circularly polarized rectenna for RF energy harvesting systems," *Int. J. RF Microw. Comput. Eng.*, vol. 29, no. 1, e21665, Jan. 2019.
[45] A. Contreras, B. Rodriguez, L. Steinfeld, *et al*., "Design of a rectenna for energy harvesting on Wi-Fi at 2.45 GHz," in *Proc. 2020 Argentine Conf. on Electronics*, Buenos Aires, 2020, pp. 63–68
[46] A. D. Boursianis, M. S. Papadopoulou, S. Koulouridis, *et al*., "Triple-band single-layer rectenna for outdoor RF energy harvesting applications," *Sensors*, vol. 21, no. 10, pp. 1–18, Oct. 2021.
[47] S. Chandravanshi and M. J. Akhtar, "An efficient dual-band rectenna using symmetrical rectifying circuit and slotted monopole antenna array," *Int. J. RF Microw. Comput. Eng.*, vol. 30, no. 4, pp. 1–15, April 2020.
[48] A. Okba, A. Takacs, and H. Aubert, "Compact rectennas for ultra-low-power wireless transmission applications," *IEEE Trans. Microw. Theory Tech.*, vol. 67, no. 5, pp. 1697–1707, May 2019.
[49] M. Aboualalaa, I. Mansour, A. B. Abdelrahman, *et al*., "Dual-band CPW rectenna for low input power energy harvesting applications," *IET Circuits, Devices Syst.*, vol. 14, no. 6, pp. 892–897, Sep. 2020.
[50] Karampatea and Siakavara, "Synthesis of rectenna for powering micro-watt sensors by harvesting ambient RF signals' power," *Electronics*, vol. 8, no. 10, p. 1108, Oct. 2019.

Mohd Hezri Abdullah was born in Kedah, Malaysia, in 1975. He received the B.Eng. degree from the University of Sheffield, UK, in 1998 and the M.Eng. degree from the Universiti Teknikal Malaysia Melaka in 2013. B.Eng is in Electronic (Communication) and M.Eng is in Electronic (Telecommunication Systems). He is currently pursuing a Ph.D. degree with the School of Electrical and Electronic Engineering, Universiti Sains Malaysia. Before that, he has been working in the Electronic and Telecommunication field for the past 21 years with the Malaysian government and multinational companies. His research interests include rectifier and antenna design, RF energy harvesting, wireless broadband technology, and fiber optics.

Arjuna Marzuki graduated with B.Eng. in Electronic Engineering from the University of Sheffield, an MSc. from Universiti Sains Malaysia, and a Ph.D. from Universiti Malaysia Perlis. He was an Associate Professor at the School of Electrical and Electronic Engineering, Universiti Sains Malaysia. He is a professional engineer registered with the Board of Engineers Malaysia and a Chartered Engineer registered with the UK Engineering Council. He is also a Fellow of the Institution of Engineering and Technology (IET). For more information, he can be contacted by email at arjunam@wou.edu.my.

Mohd Tafir Mustaffa received his B. Eng degree in electrical and electronic engineering from Universiti Sains Malaysia (USM), Penang in 2000. He was awarded a master's degree (M. Eng. Sc) in computer and microelectronic engineering from Victoria University, Australia in 2005 and officially completed his Ph.D. degree in electrical engineering specializing in radio frequency integrated circuits (RFIC) in September 2009. He served as a system engineer at Data Acquisition System (M) Sdn. Bhd. and tutor in USM. He is now a senior lecturer at the School of Electrical and Electronic Engineering, USM Engineering Campus. Mohd Tafir Mustaffa is a Senior Member of IEEE; actively involved with IEEE Circuits and Systems Society for the last few years as a committee member. He is the author and co-author of close to 50 technical papers in conferences and journals, books, and book chapters. He was a recipient of the IETE J C Bose Memorial Award in 2017. He is currently involved in the research of analog IC, RFIC, and RF MEMS design.